Simulation of surface temperature inversions in complex terrain and implementation of slope irradiance

Gard Hauge *(Corresponding author)*
Geophysical Institute, University of Bergen, Allégt. 70, 5007 Bergen, Norway
www.gfi.uib.no • email: gard.hauge@gfi.uib.no

Lars R. Hole
Norwegian Institute for Air Research, Norway
www.nilu.no • email: lrh@nilu.no

Abstract

The atmospheric mesoscale model MM5 has been used at high horizontal resolution to simulate the break-up of a temperature inversion in complex topography. To improve the surface parameterisations during daytime, slope and orientation of the terrain has been taken into account in the calculation of SW radiation at the surface. Compared to observations, results show improvement in both temperature and wind fields after the implementation of slope irradiances in MM5. The break-up part of the temperature inversion is also simulated more correctly. The RMS error is reduced by 35% for wind speed and 13% for temperature.

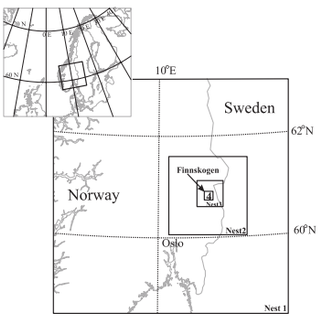

Fig. 1: Nesting of MM5 domains. All domains are 40 x 40 grid points with the resolution from 13.5 km nested down to 500 meters resolution. The upper left figure shows the position of Nest 1 on a European scale.

Implementation of slope irradiance

Slope irradiance can normally be neglected in numerical models when the horizontal model resolution is low (O (10) km or more) and the slopes are moderate. On the other hand, when the resolution is higher (O (1) km), the effect of slopes might be considerable, especially at low solar zenith-angles and at high latitudes. Slope irradiance should therefore be included when the resolution becomes high and the terrain steep and undulating. SW radiation at the surface is originally calculated under the assumption of horizontal surfaces (Dudhia, 1989), i.e. SW radiation at the surface is a dependent of the solar height, h, and a function, F, depending on transmissivity, water vapour, clouds and scattering, given as:

$$S = S_0 \sin(h) F \qquad (1)$$

S0 is the solar constant, depending on the mean distance and the actual distance to the sun.
The solar elevation is given as:

$$\sinh = \sin\delta \sin\varphi - \cos\delta \cos\varphi \cos\Omega\,, \qquad (2)$$

where δ is Earth's declination, φ is geographic latitude in degrees (north positive) and Ω is the hour angle.

We have to split the global irradiance into its direct and diffuse components in order to describe the slope irradiance. This splitting is done according to a method developed by Skartveit and Olseth (1987), valid at high latitudes (> 30 degrees) and implemented into MM5. When slope and orientation of the surface (the topography-azimuth angle), and the hourly diffuse and beam irradiances, S_B and S_D, on a horizontal surface, are known, the total irradiance on a surface inclined by an angle β towards an azimuth angle γ (orientation) can be written:

$$S(\beta,\gamma) = S_B \frac{\cos(\theta)}{\sin(h)} + (1-\cos^2\frac{\beta}{2})\alpha(S_D + S_B) + S_D(\alpha,\gamma)\,, \qquad (3)$$

where h is solar elevation, β is ground slope (calculated using forward differences), and θ is the solar beam angle of incidence. The term

$$(1-\cos^2\frac{\beta}{2})\alpha(S_D + S_B)$$

is ground reflected irradiance. Negative θ is replaced by zero in (3). The solar beam angle of incidence can be written as (Skartveit and Olseth, 1986):

$$\cos(\theta) = \cos(h)\sin\beta\cos(\psi-\gamma) + \sin(h)\cos\beta\,, \qquad (4)$$

which explains the correspondence between solar radiation and orientation and slope of the underlying terrain. The solar azimuth is ψ where south is zero and east is positive.

For further details, see Hauge and Hole (2002).

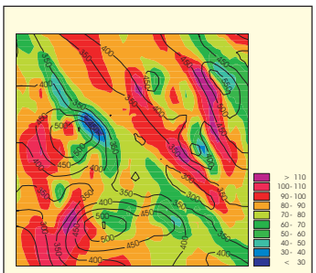

Fig. 2: (a): Net incoming SW radiation in the modified run. Legend on the right shows W/m², lines are topography. The domain is 20 x 20 km and has a 500-meter grid distance in the MM5 simulation.

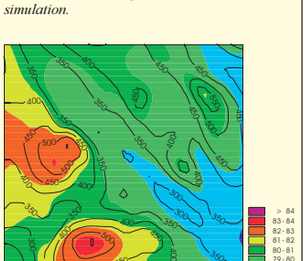

Note the difference of scales on the two figures.

Model configuration and observations

First-guess fields are produced by interpolating data from ECMWF (European Centre for Medium Range Weather Forecast) to the outer computational grid (13.5 km), and nested down to 500 meters horizontal grid distance (see Fig. 1). The number of grid-points were 40x40 for all domains and 31 vertical layers. The 31 vertical sigma levels are spaced so as to provide much higher vertical resolution in the planetary boundary layer than at upper levels (13 layers below 1000 meters).

In the present simulations, the turbulence scheme based on Hong and Pan (1996) is used, coupled to the OSULSM (Chen and Dudhia (2001a, 2001b)). An explicit moisture scheme, including the ice phase, was used (Dudhia, 1989). The radiation scheme applied, based on Dudhia (1989), has been modified to take into account the effect of sloping surfaces. For the outer domain (grid distance 13.5 km), a cumulus parameterisation based on Grell et al. (1989) has been used.

In order to evaluate and compare model results with measured data, a situation from 21 September 1994 was chosen (Hole et al. (1998)). The geographical area of interest has been Finnskogen in Hedmark County, NE of Oslo. In this area, the ground is undulating and mostly covered with conifer forest, but the observation site is relatively flat (2-3 degrees). To test the effect of the changes made in the radiation scheme, two model runs are conducted. The first, called the *reference-run*, used the original SW parameterisations, and the second, called the *modified run*, had slope irradiance implemented.

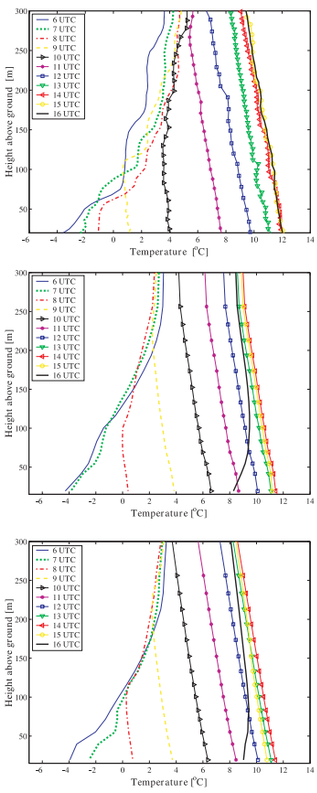

Fig. 3: (a) Observed temperature soundings from 06 UTC to 16 UTC.
(b) Modelled soundings in the reference run at 500 m grid distance.
(c) Modelled temperature soundings in the modified run.

Model results - effects of slope irradiance

Effects of slope irradiance in the finest domain (500 m grid distance) on the net incoming SW radiation are shown in Fig. 2. There is evidently more SW radiation in the modified run on slopes oriented towards the sun and less in shadow areas, and the effects of slope irradiance are enhanced in steeper areas. Observed soundings are shown in Fig. 3a, revealing a classical example of a morning temperature inversion break-up. The figure clearly demonstrates how the ground was heated by solar radiation and how statically unstable air close to ground penetrates deeper into the inversion layer and destroys it from below. The soundings taken from MM5 are based on the 500-meter grid distance, and the changes in the modified temperature soundings compared to the reference run are shown in Fig. 3b and 3c. Largest differences are mostly seen in the morning and in the afternoon near the surface.

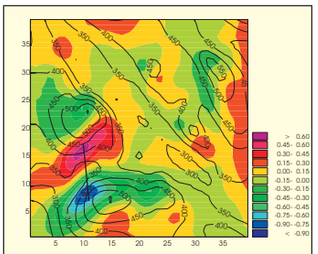

Fig. 5: (a) Difference in temperature at the lowest model layer (20 meter) between the modified run and the reference run at 09 UTC ($T_{modified}$-$T_{reference}$). Negative values are therefore showing cooler areas in the modified run, and positive warmer areas. The line shows the cross-section on Fig. 3b. Ticks on axis shows grid point numbers, where each corresponds to 500 meters.

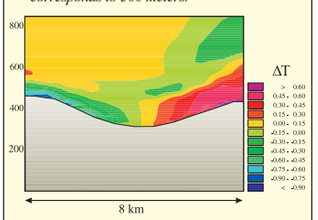

(b) Cross-section of the temperature difference between the modified and reference run indicated on (a). On the vertical axis is height above sea level.

The soundings are slightly too warm in both simulations in the middle of the day and too cold in the afternoon, compared to observations. The modified run seems to give a more accurate break-up of the temperature inversion. In the afternoon, the observation area is oriented to southwest, giving less cooling than in the reference-run. This effect gives a slower formation of a new inversion and is more according to the observations. The effect on temperatures in the observation point of slope irradiance is not large, and the reason for this is mostly due to small terrain gradients 2-3 degrees in this area.

In the reference winds are too low, while there are evident improvements in the modified run (Fig. 4). Temperature differences between the modified and the reference run in the lowest model layer (20 m) at 09 UTC are shown in Fig. 4a. The solar height is low, and the largest cross-valley temperature difference ranges up to 1.5 degrees. The line indicated on Fig. 4a is the cross section shown in Fig. 4b, and vertical effects are seen 200 meters above ground in this area. Results were changed circulation patterns, with rising motion at the sun side and descending air at the shadow side of the valley (not shown).

Error statistics and concluding remarks

To evaluate the model results of wind speed and temperature, the root mean square errors (RMSE) have been computed. The RMSE shown on Fig. 6 is based on the interpolated temperatures and wind speeds from 10 to 300 meters from 06 UTC to 16 UTC. The statistical analysis is done in discrete levels from 10 to 300 meters, and the RMSE at each level is calculated on the based on the observations from 06 UTC to 16 UTC (11 values at each level). After the modification, the daily temperature variation has better correspondence to observations, especially in the morning and in the afternoon. The implementation of slope irradiances reduced the mean RMSE in temperature by 13%. Mean RMSE for the wind fields are reduced with 35%. The larger differences in wind speed speeds can be caused by local circulation patterns. Temperature near the surface has close dependency on the local physical grid-point properties such as Aledo and emissivity, while the effects on the wind fields easier can be advected to other areas. Circulation set up in steeper areas can therefore have larger influence in other areas of the domain. These results suggest that influence of slope irradiance is greater on the wind fields than on the temperature fields.

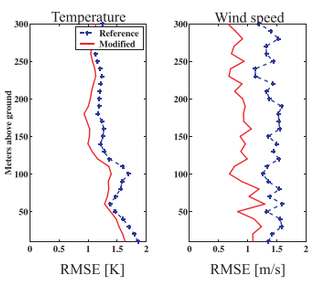

Fig. 6: Left: RMSE in temperature between 06 UTC and 16 UTC. Right: RMSE in wind speed.

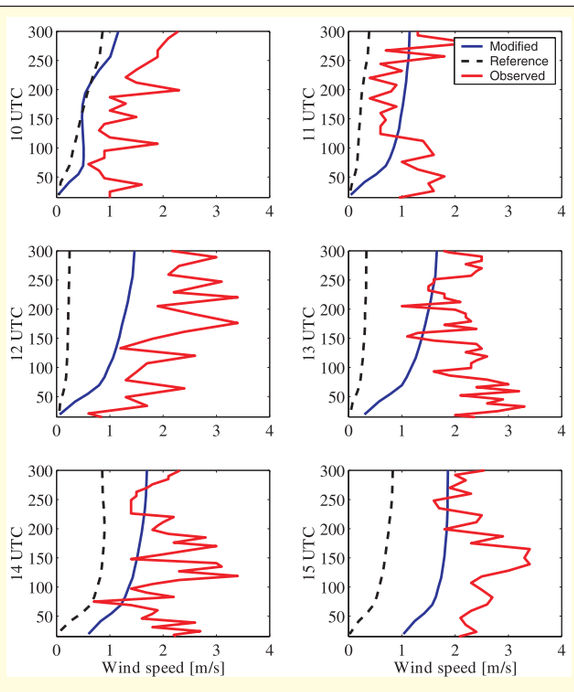

Fig. 4: Observed and modelled wind speed from 10 to 15 UTC. Red lines are observed, blue the modified run, and the dotted black line are the reference run.

References

Chen F, Dudhia J. *Coupling an advanced land-surface/hydrology model with the Penn State/NCAR MM5 modelling system. Part 1: Model implementation, and sensitivity.* Monthly Weather Review 2001a; 129: 569-585.

Chen F, Dudhia J. *Coupling an advanced land-surface/hydrology model with the Penn State/NCAR MM5 modelling system. Part 2: Preliminary model validation.* Monthly Weather Review 2001b; 129: 587-604.

Dudhia, J. *Numerical study of convection observed during the winter monsoon experiment using a mesoscale two-dimensional model.* J. Atmos. Sci., 1989: 46(20), 3077—3107.

Grell G, Dudhia J, Stauffer D. *A description of the fifth-generation Penn-State/NCAR mesoscale model.* NCAR technical report note TN-398, National Center for Atmospheric Research, Boulder Colorado, US, 1994.

Hauge G, Hole L R. *Implementation of slope irradiance in MM5 and its effect on temperature and wind fields during the break-up of a temperature inversion.* Submitted Journal of Geophysical Research May 2002.

Hole L.R, Gjessing Y, de Lange T. *Meteorological measurements and conditions during Norwegian Trials. Measurements During Summer and Winter Conditions.* Noise 1998; 46(5) (Special issue):199-207.

Hong S, Pan H. *Non-local boundary layer vertical diffusion in a medium range forecast model.* Monthly Weather Review 1982; 214(2): 2322-2339.

Skartveit A, Olseth J. *Modelling slope irradiance at high latitudes.* Solar Energy 1986; 36(4): 333-344.

Skartveit A, Olseth J. A *model for the diffuse fraction of hourly global radiation.* Solar Energy 1987; 38(4): 271-274.

Stull R.B, *An introduction to boundary layer meteorology.* Kluwer Academic Publishers, Boston, USA, pp. 379-381, 1988.